Journal of Hydraulic Research

ISSN: 0022-1686 (Print) 1814-2079 (Online) Journal homepage: http://www.tandfonline.com/loi/tjhr20

Eigenfrequency shift mechanism due to variation in the cross sectional area of a conduit

Moez Louati & Mohamed S. Ghidaoui

To cite this article: Moez Louati & Mohamed S. Ghidaoui (2017): Eigenfrequency shift mechanism due to variation in the cross sectional area of a conduit, Journal of Hydraulic Research, DOI: 10.1080/00221686.2017.1394373

To link to this article: https://doi.org/10.1080/00221686.2017.1394373

Journal of Hydraulic Research, 2017
https://doi.org/10.1080/00221686.2017.1394373

Eigenfrequency shift mechanism due to variation in the cross sectional area of a conduit

MOEZ LOUATI (IAHR Member), Post-Doctoral Fellow, *Civil and Environmental Engineering/School of Engineering, The Hong Kong University of Science and Technology, Kowloon, Hong Kong, PR China*
Email: mlouati@connect.ust.hk (author for correspondence)

MOHAMED S. GHIDAOUI (IAHR Member) Chair Professor, *Civil and Environmental Engineering, The Hong Kong University of Science and Technology, Kowloon, Hong Kong, PR China*
Email: ghidaoui@ust.hk

ABSTRACT
Eigenfrequency (i.e. natural resonant frequency) shift due to variation in the cross sectional area of a conduit is observed in different applications such as vocal tracts, musical instruments and water supply systems. In the context of water supply systems, past research focused on developing inverse problem techniques that use shifts in eigenfrequencies to identify blockages. The goal of this paper is to understand the mechanisms that cause this eigenfrequency shift. Application of the principle of action invariance to a small blockage shows that the eigenfrequency shift is directly related to the change in energy. For a severe blockage, the pipe system is decoupled into two independent subsystems: a subsystem that involves the blockage and another that involves the intact pipe section. The decoupling is lost when the blockage length is such that the fundamental frequencies of the two subsystems are close or equal, resulting in resonance where perturbation theory is successfully used to derive a simple frequency relation.

Keywords: Asymptotic approach; blockage-detection in pipe system; eigenfrequency shift mechanism; energy approach; transient flow; pipe system

1 Introduction

The possibility of using a measured pressure trace to infer the internal shape of a conduit is of interest to vocal tract and water supply researchers. In particular, it is found that the eigenfrequencies (i.e. natural resonant frequencies) of a measured pressure signal vary with the cross sectional area of the conduit (De Salis & Oldham, 1999; Domis, 1980, 1979; Duan, Lee, Ghidaoui, & Tung, 2012; Fant, 1975; Heinz, 1967; Mermelstein, 1967; Milenkovic, 1987, 1984; Qunli & Fricke, 1990, 1989; Schroeder, 1967; Schroeter & Sondhi, 1994; Sondhi & Gopinath, 1971; Sondhi & Resnick, 1983; Stevens, 1998). The interrelation between eigenfrequencies and the cross sectional area of a conduit has been recently used to formulate algorithms for defect detection in water supply systems (e.g. Zhao, Ghidaoui, Louati, & Duan, in press; Duan et al., 2012; Duan et al., 2013; Lee, Duan, Ghidaoui, & Karney, 2013; Lee, Vítkovský, Lambert, Simpson, & Liggett, 2008; Louati, 2013; Louati & Ghidaoui, 2015; Meniconi et al., 2013; Mohapatra, Chaudhry, Kassem, & Moloo, 2006; Sattar, Chaudhry, & Kassem, 2008; Wang, Lambert, & Simpson, 2005). These research activities are motivated by the fact that blockages are ubiquitous in water supply systems and their presence is costly and wastes energy.

The importance of developing detection algorithms for blockages meant that the focus of past research is on the inverse problem where mathematical relations that link the eigenfrequencies to the cross sectional area of the pipe are formulated and algorithms for how these relationships can be used to infer blockages from measured eigenfrequencies are proposed (e.g. Duan et al., 2012; Duan et al., 2013; Lee et al., 2013; Meniconi et al., 2013). While this research direction is promising and has led to proof of concept under idealized laboratory settings, there are a number of unresolved issues. For example, there is no proof that the inverse problem, which relates the unknown blockage properties to the measured eigenfrequencies, has a unique solution, nor is there a technique to find it even if it exists. In fact, current solutions of this inverse problem require that the number of blockages is known a priori, which is unrealistic in practice. In addition, the computational time needed to solve the inverse problem grows with the number of blockages.

Received 10 February 2016; accepted 16 October 2017/Currently open for discussion.

ISSN 0022-1686 print/ISSN 1814-2079 online
http://www.tandfonline.com

The area of vocal tract reconstruction, which shares many similarities, including the governing equations, with the problem of blockage detection in pipes, has made progress instead by seeking to better understand the forward problem, using this improved understanding to develop robust inversion techniques. For example, Mermelstein (1967) showed that the eigenfrequency (i.e. natural resonant frequency) shift of the *m*th pressure mode is directly linked to the amplitude of the *m*th term in the Fourier series expansion of the cross sectional area function of the conduit with respect to longitudinal distance, and showed how this relationship can be imposed as a constraint that guarantees uniqueness of the inverse problem. In addition, Schroeder (1967) showed that the Ehrenfest theorem (Ehrenfest, 1916) can be used to formulate an algorithm for determining the geometry of the vocal tract from measured values of the eigenfrequencies of the acoustic pressure wave. Schroeder's (1967) results formed the basis of a number robust algorithms to solve the inverse problem in the vocal tract field (e.g. Fant, 1975; Schroeter & Sondhi, 1994; Sondhi & Gopinath, 1971; Sondhi & Resnick, 1983; Stevens, 1998) and other fields (e.g. De Salis & Oldham, 1999; Domis, 1980, 1979; Milenkovic, 1987, 1984; Qunli & Fricke, 1990, 1989). El-Rahed and Wagner (1982) investigated the forward problem of blockage-acoustic wave interaction in finite cylindrical cavities and concluded that one-dimensional wave theory is acceptable for a large blockage, while details of the acoustic field are revealed only by three-dimensional analysis.

This paper constitutes a first attempt to shed greater light on the forward problem, as if this forward problem is understood, the issues that arise in connection with its inversion can be addressed. In particular, the aim is to understand the interaction between a blockage and the eigenfrequencies. The theoretical model considered in this work consists of a reservoir-pipe-valve (RPV) system containing a single blockage with different radial and longitudinal extent. A blockage in this paper is defined only by a location, a length and a radial extent as these are the main parameters that contribute to the eigenfrequency shift mechanism. The remainder of the paper is structured as follows. The problem statement is given in Section 2. The case of small variation in the cross sectional area is discussed in Section 3 where the energy approach is used to describe the different aspects of the eigenfrequency shift. Section 4 discusses the cases of severe cross sectional area variation in which the asymptotic approach is introduced. In Section 5, moderate variation in the cross sectional area is discussed. Finally, conclusions are drawn in Section 6.

2 Problem statement

The eigenfrequency shift mechanism is studied for the simple case of a RPV system as shown in Fig. 1. The blocked pipe system is modelled as the junction of two pipes in series with different diameters (Fig. 1). The two pipes are defined as

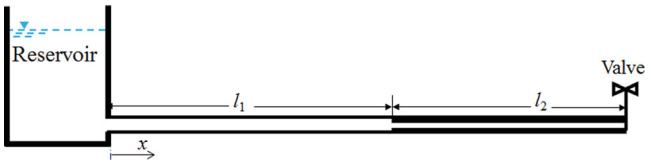

Figure 1 Reservoir-pipe-valve system with change in cross-sectional area

pipe 1 with length l_1 and cross sectional area $A_1 = A_0$ and pipe 2 with length l_2 and cross sectional area $A_2 < A_0$ where A_0 is the intact cross sectional area. Pipe 2 represents the blockage. The ratio between the cross sectional of the blocked and intact pipe is $\alpha = A_2/A_0$. The dimensionless lengths are defined by x/L, $\eta_1 = l_1/L$ and $\eta_2 = l_2/L$ where $L = l_1 + l_2$ is the total length of the blocked pipe system and x is the distance along the pipe length from the reservoir (Fig. 1).

A one-dimensional model is used to represent the pressure and flow variations and it is assumed that the fluid is inviscid. Moreover, the change in wave speed due to the blockage is neglected in this work because (i) the wave speed variation is usually small for shallow and/or discrete blockage; and (ii) it does not change the mechanism of eigenfrequency shift, which is the main purpose of this work. It is important to notice that the change in eigenfrequencies does not depend on the head loss caused by a blockage in a real system. Therefore, the head loss due to the presence of a blockage is neglected in this work. In what follows, a case without blockage such that $\alpha = 1$ is referred as an *intact* pipe case.

Applying the transfer matrix method (Chaudhry, 2014) on the blocked pipe system in Fig. 1, the dispersion relation that relates the natural resonant frequencies (eigenfrequencies) of the system to its characteristics (e.g. length, diameter, wave speed) could be obtained. This dispersion relation depends mainly on the boundary condition (BC) of the system. For the case of the blocked pipe system in Fig. 1, the dispersion relation is given by:

$$\cos(k_m l_2)\cos(k_m l_1) - \alpha \sin(k_m l_2)\sin(k_m l_1) = 0; \quad m = 1, 2, 3 \ldots \tag{1}$$

where $k_m = w_m/a$ is the wavenumber of the *m*th fundamental (resonant) mode and a is the acoustic wave speed. A generalized form of the dispersion relation for the case of multiple blockages can be found in Duan et al. (2012). Trigonometric manipulation of Eq. (1) gives:

$$\cos(k_m L) + (1 - \alpha)\sin(k_m l_2)\sin(k_m l_1) = 0 \tag{2}$$

Note that the second term in Eq. (2) represents the effect of the blockage on the dispersion relation. In fact, for $\alpha = 1$, this second term vanishes and Eq. (2) becomes identical to the dispersion relation of an intact RPV system ($\cos(k_m L) = 0$).

Equation (1) is used to study the variation of the eigenfrequencies (w_m). Figure 2 plots the eigenfrequency variation with dimensionless length $\eta_2 = l_2/L$ for the first four modes ($m = 1$,

2, 3 and 4) and for different values of α. Since $\alpha = 1$ represents the eigenfrequencies of the intact pipe case, these eigenfrequencies are independent of η_2 and are shown as horizontal lines in Fig. 2. When $\alpha \neq 1$, the second term on the left hand side of Eq. (2) is not identical to zero. Therefore, the eigenfrequency at a given mode m (w_m) deviates from its intact case (w_m^0) (Fig. 2). In fact, Fig. 2 shows that the eigenfrequencies for $\alpha \neq 1$are oscillating with respect to the eigenfrequencies of the intact case (w_m^0). The eigenfrequency shift $\Delta w_m = (w_m - w_m^0)$ takes positive values for some range of blockage length η_2, negative values for some range of blockage length η_2, and equals zero for particular values of blockage length η_2.

In addition, Fig. 2 shows that the eigenfrequency shift (Δw_m) becomes pronounced with the severity of the blockage (i.e. as α gets smaller), except for some special values of η_2 where the eigenfrequency shift is zero regardless of the severity of the blockages. Furthermore, Fig. 2 shows that for $\eta_2 \neq 1/2$, the maximum eigenfrequency shift occurs at different blockage lengths as the blockage severity increases (i.e. the value of η_2 at which Δw_m is an extremum varies with α). On the other hand, Δw_m reaches its extremum at $\eta_2 = 1/2$ regardless of the value of α.

For better understanding of Fig. 2, Fig. 3 gives the frequency response function of pressure measurement at the valve prior to transient generated by a sudden open-close of the valve for the case where $\eta_2 = 1/3$ and $\alpha = 0.2$. The shifts of the eigenfrequencies are clear in Fig. 3. The first and fourth eigenfrequencies experience positive shift, whereas the second and third eigenfrequencies experience zero and negative shifts, respectively. The primary objective of this paper is to provide physical and

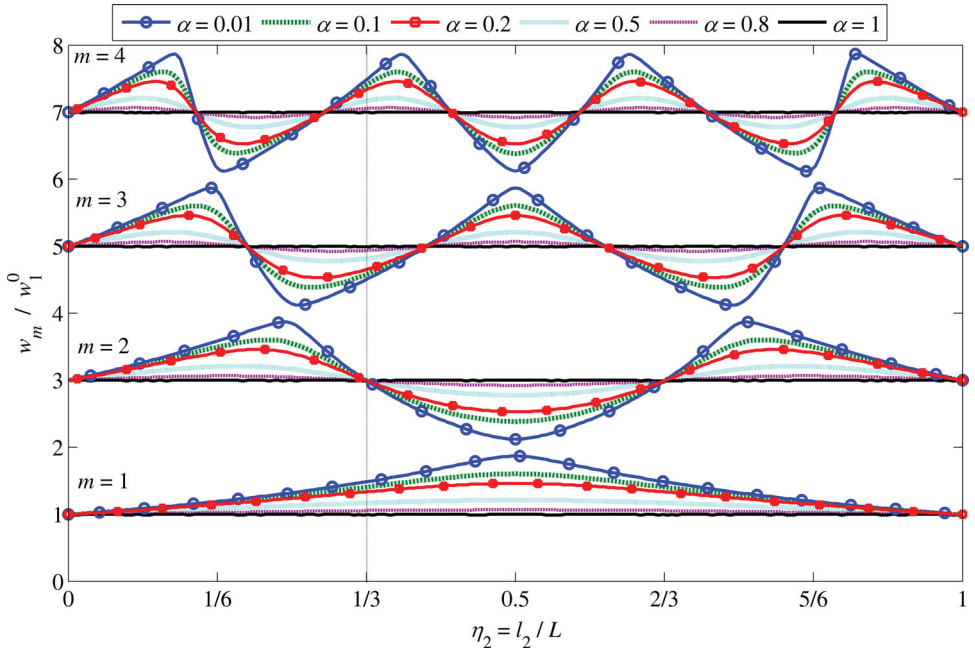

Figure 2 Dimensionless eigenfrequency variation with dimensionless length η_2 of the first four modes for different α values

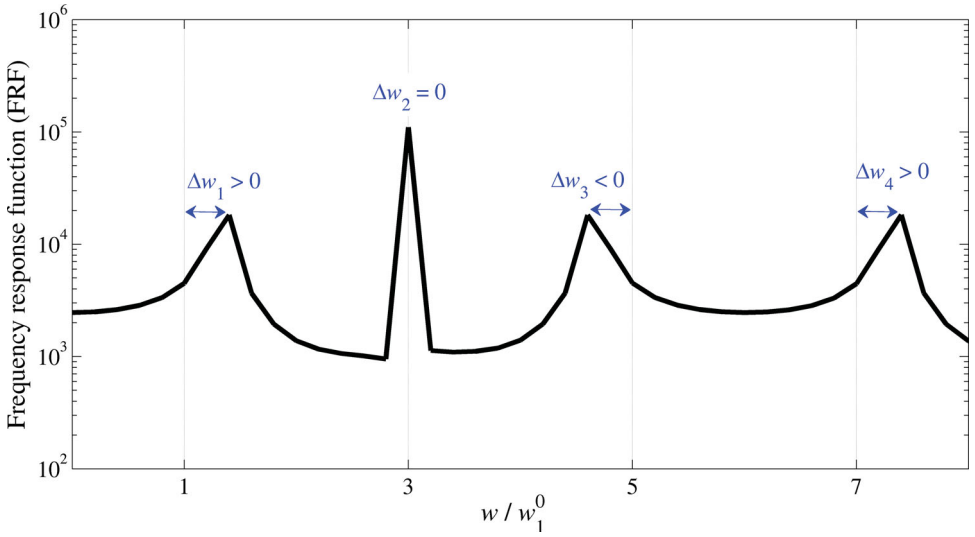

Figure 3 Frequency response function of pressure measurement at the valve for the case where $\eta_2 = 1/3$ and $\alpha = 0.2$

mathematical insights that can explain the above observations that emerge from Fig. 2. Such understanding is presently lacking; yet, this insight is essential if the dispersion relation (Duan et al., 2012) is to become a viable approach for identifying blockages in fluid lines.

3 Analysis and discussion of frequency-blockage interaction for blockage with small radial protrusion (i.e. α near 1)

3.1 *Relationship between eigenfrequency shift and change in energy*

The principle of action invariance, which states that the action is invariant for processes whose time scale (i.e. process time for the blockage to be created) is significantly larger than the period of oscillations (i.e. transient time), was successfully used by Schroeder (1967) to show that the shift in frequency due to change in area in a vocal tract is related to the change in total energy brought about by the work done on air by the contraction and expansion of the vocal tract. In this section, the principle of action invariance is applied to the blockage shown in Fig. 1. Notice that "action" (used above) is usually defined (in classical physics) as the integral over time of the difference between kinetic and potential (elastic) energy. This goes back to the action principles (e.g. principle of least action) (Lanczos, 2012). The derivation that follows is along the lines of that proposed by Fant (1975).

The elastic potential energy (U_m) and kinetic energy (T_m) per unit length for the mth mode are (Karney, 1990):

$$U_m = \frac{\rho A_0}{2}\left(\frac{g}{a}\right)^2 h_m^2; \quad T_m = \frac{\rho}{2}A_0 V_m^2 = \frac{\rho}{2A_0}q_m^2; \quad E_m = U_m + T_m = \frac{\rho A_0}{2}\left[\left(\frac{g}{a}\right)^2 h_m^2 + \frac{q_m^2}{A_0^2}\right] \tag{3}$$

where h_m, q_m and V_m are the unsteady pressure head, flow discharge and flow velocity for the mth mode (see Appendix 1), respectively; ρ is the fluid density; U_m, T_m and E_m are elastic potential energy, kinetic energy and total energy for the mth mode, respectively; a is the acoustic wave speed; g is the standard gravitational acceleration constant; and A_0 is the intact cross sectional area of the pipe.

Short (discrete) blockage

Consider a short section of the blockage with length Δx and with radial extent small enough that the associated changes in head and flow rate are small and can be neglected (i.e. the harmonic solutions of pressure and flow (see Appendix 1) are almost unchanged due to a blockage with small radial extent (Fig. 4)). As a result, the changes in kinetic, potential and total energies per unit length of mode m are:

$$\Delta U_m = \frac{\rho}{2}\Delta A\left(\frac{g}{a}\right)^2 h_m^2; \quad \Delta T_m = -\frac{\rho \Delta A}{2A_0^2}q_m^2;$$
$$\Delta E_m = \frac{\rho}{2}\Delta A\left[\left(\frac{g}{a}\right)^2 h_m^2 - \frac{q_m^2}{A_0^2}\right] \tag{4}$$

where $\Delta A = A_2 - A_0 \leq 0 = (\alpha - 1)A_0$. Equation (4) shows that a small localized blockage increases the kinetic energy and, conversely, reduces the elastic potential energy. To explain, the blockage occupies some space that was occupied by the fluid prior to the formation of the blockage. Therefore, the mass of the fluid in the blockage region is smaller by a factor of $(1 - \alpha)$ than the mass that was there before the blockage was formed. Since the change in head due to the small blockage is negligible (Fig. 4), the reduction of mass by a factor of $(1 - \alpha)$ results in reduction in elastic potential energy by the same factor. Since the change in flow rate due to the small blockage is negligible (Fig. 4), the flow velocity at the blockage is $1/\alpha$ times the flow velocity without the blockage. The reduction in mass and

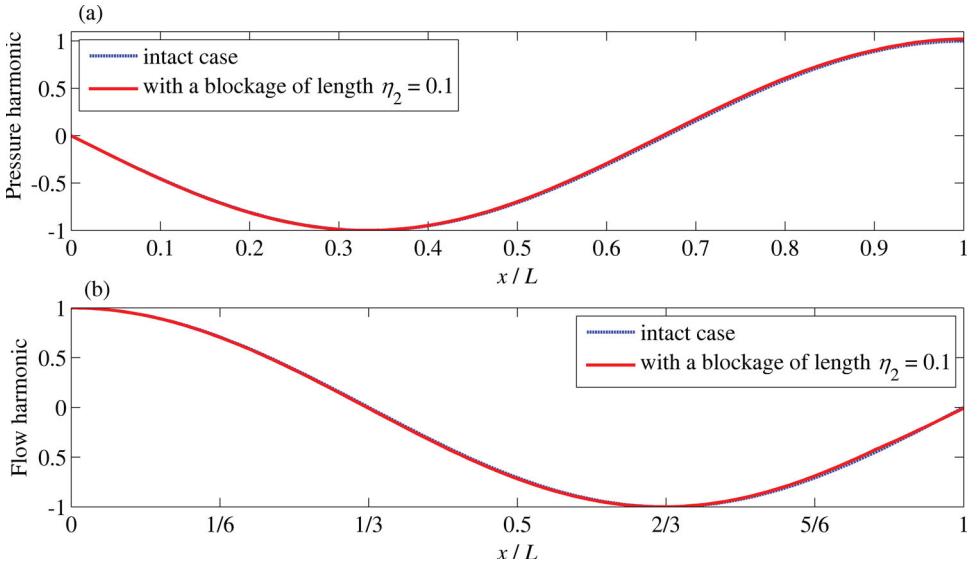

Figure 4 Pressure head (a) and flow rate (b) harmonics variation for small blockage ($\alpha = 0.9$)

increase in velocity due to the blockage results in an increase in kinetic energy by a factor of $1/(1-\alpha)$.

The explicit dependence of energy on frequency is brought about by considering the momentum and continuity equations (see Appendix 1):

$$iwq_m^0 = -gA_0\frac{dh_m^0}{dx} \tag{5}$$

$$iwh_m^0 = -\frac{a^2}{gA_0}\frac{dq_m^0}{dx} \tag{6}$$

where $i=\sqrt{-1}$. Therefore, the kinetic energy for the cases with and without blockage can be calculated as:

$$T_m^0(w_m^0) = \frac{\rho}{2A_0}(q_m^0)^2 = -\frac{1}{(w_m^0)^2}\frac{\rho A_0 g^2}{2}\left(\frac{dh_m^0}{dx}\right)^2 \tag{7}$$

$$\begin{aligned} T_m^I(w_m^I) &= T_m^0(w_m^0) + \Delta T_m \\ &= -\left[1+\frac{\Delta A}{A_0}\right]\frac{1}{(w_m^I)^2}\frac{\rho A_0 g^2}{2}\left(\frac{dh_m^0}{dx}\right)^2 \end{aligned} \tag{8}$$

where w_m^0 is the mth eigenfrequency for the case without blockage, and w_m^I is the mth eigenfrequency for the case with blockage that would result from the change in kinetic energy only.

Dividing Eq. (7) by Eq. (8) yields:

$$\frac{(w_m^I)^2}{(w_m^0)^2} = \left(1+\frac{\Delta A}{A_0}\right)\frac{T_m^0}{T_m^0+\Delta T_m} \tag{9}$$

While the change in kinetic energy shifts the frequency of mode m from w_m^0 to w_m^I, the change in elastic potential energy shifts the frequency of the same mode from w_m^I to w_m^{II}. Therefore, we obtain:

$$U_m^I = \frac{\rho A_0}{2}\left(\frac{g}{a}\right)^2(h_m^0)^2 = -\frac{1}{(w_m^I)^2}\frac{\rho a^2}{2A_0}\left(\frac{dq_m^0}{dx}\right)^2 \tag{10}$$

$$U_m^{II} = U_m^I(w_m^I) + \Delta U_m = -\left[1-\frac{\Delta A}{A_0}\right]\frac{1}{(w_m^{II})^2}\frac{\rho a^2}{2A_0}\left(\frac{dq_m^0}{dx}\right)^2 \tag{11}$$

Dividing Eq. (10) by Eq. (11) yields:

$$\frac{(w_m^{II})^2}{(w_m^I)^2} = \left(1-\frac{\Delta A}{A_0}\right)\frac{U_m^I}{(U_m^I+\Delta U_m)} \tag{12}$$

Multiplying Eq. (9) with Eq. (12) yields:

$$\frac{(w_m^{II})^2}{(w_m^0)^2} = \frac{[1-(\Delta A/A_0)^2]}{\left(1+\frac{\Delta U_m}{U_m^I}\right)\left(1+\frac{\Delta T_m}{T_m^0}\right)} \approx \frac{1}{\left(1+\frac{\Delta U_m}{U_m^I}\right)}\frac{1}{\left(1+\frac{\Delta T_m}{T_m^0}\right)} \tag{13}$$

Since a small blockage results in small change in energy, Eq. (13) can be rewritten as:

$$\begin{aligned} \frac{(w_m^{II})^2}{(w_m^0)^2} &= \left(1-\frac{\Delta U_m}{U_m^I}\right)\left(1-\frac{\Delta T_m}{T_m^0}\right) \Rightarrow \frac{w_m^{II}}{w_m^0} \\ &= \left(1-\frac{\Delta U_m}{U_m^I}\right)^{1/2}\left(1-\frac{\Delta T_m}{T_m^0}\right)^{1/2} \end{aligned} \tag{14}$$

Using Taylor expansion and neglecting second order terms, Eq. (14) becomes:

$$\frac{w_m^{II}}{w_m^0} = 1-\frac{1}{2}\left(\frac{\Delta U_m}{U_m^I}+\frac{\Delta T_m}{T_m^0}\right) \tag{15}$$

The equipartition theorem for linear wave problems states that (Mei, Stiassnie, & Yue, 2005):

$$U_m^I(w_m^I) = T_m^0(w_m^0) = \frac{E_m^0}{2} \tag{16}$$

where E_m^0 is the total energy of the mode m for the case without blockage. Inserting Eq. (16) into Eq. (15) yields:

$$\begin{aligned} \frac{w_m^{II}}{w_m^0} &= 1-\left(\frac{\Delta U_m}{E_m^0}+\frac{\Delta T_m}{E_m^0}\right) \Rightarrow \frac{w_m^{II}-w_m^0}{w_m^0} \\ &= -\frac{(\Delta U_m+\Delta T_m)}{E_m^0} \Leftrightarrow \frac{\Delta w_m}{w_m^0} = -\frac{\Delta E_m}{E_m^0} \end{aligned} \tag{17}$$

where Δw_m and $\Delta E_m$are the eigenfrequency shift and the change in energy due to the blockage of the mth mode, respectively. The same relation arises in many areas such as quantum mechanics, where it is referred to as the Ehrenfest theorem (Ehrenfest, 1916), and classical mechanics (e.g. oscillations of pendulums (Beyer, 1978) and acoustic waves in vocal tracts (Schroeder, 1967)). Using Eq. (4), Eq. (17) becomes:

$$\begin{aligned} \frac{\Delta w_m}{w_m^0} &= -\frac{\Delta E_m}{E_m^0} = -\frac{\rho\Delta A}{2E_m^0}\Delta x\left[\left(\frac{g}{a}\right)^2(h_m^0)^2-\left(\frac{q_m^0}{A_0}\right)^2\right] \\ &= \left(\frac{|\Delta U_m|}{E_m^0}-\frac{|\Delta T_m|}{E_m^0}\right) \end{aligned} \tag{18}$$

It is clear from Eq. (18) that Δw_m is proportional to w_m^0. Thus, the eigenfrequency shift Δw_m will only become visible for very large frequencies w_m^0. Such high frequencies cannot be generated by mechanical devices such as valves and are susceptible to viscous dissipation even if they could be generated. It is for this reason that the focus in the literature is to develop detection methods for discrete blockages on the basis of local damping that such blockages generate (e.g. Nixon & Ghidaoui, 2007; Wang et al., 2005) rather than on the basis of the small frequency shift that they produce.

Extended blockage

The eigenfrequency shift due to extended blockage such as the one shown in Fig. 1 is determined by integrating Eq. (18) along the pipe as follows:

$$\frac{\overline{\Delta w_m}}{w_m^0} = \frac{\int_0^L \Delta w_m dx}{w_m^0} = -\int_0^L \frac{\Delta E_m}{E_m^0} dx = -\frac{\rho}{2E_m^0}\Delta A \int_{l_1}^{L} \Delta x \left[\left(\frac{g}{a}\right)^2 (h_m^0)^2 - \frac{(q_m^0)^2}{A_0^2}\right] dx \quad (19)$$

where $\overline{\Delta w_m}$ and $\Delta\overline{E_m}$ are the shift in eigenfrequency and the change in energy due to the extended blockage, respectively. Note that ΔA came out from under the integral because it is a constant for the example being considered (Fig. 1). The pressure head and discharge solution for an intact RPV system are (see Appendix 1):

$$\begin{cases} h_m(x, k_m^0) = 2iC\sin(k_m^0 x) = h_m^{\text{amp}}\sin(k_m^0 x) \\ q_m(x, k_m^0) = -2C\frac{g}{a}A_0\cos(k_m^0 x) = q_m^{\text{amp}}\cos(k_m^0 x) \end{cases} \quad (20)$$

where C is a complex constant of integration; h_m^{amp} and q_m^{amp} are the mth maximum complex amplitudes of pressure head and flow discharge, respectively. Inserting Eq. (20) into Eq. (3) gives:

$$E_m^0 = \frac{\rho L A_0}{2}\left(4|C|^2\left(\frac{g}{a}\right)^2\right) = \frac{\rho L}{2A_0}|q_m^{\text{amp}}|^2 = \frac{\rho L A_0}{2}\left(\frac{g}{a}\right)^2 |h_m^{\text{amp}}|^2 \quad (21)$$

and inserting Eq. (21) into Eq. (18) yields:

$$\frac{\overline{\Delta w_m}}{w_m^0} = -\frac{\overline{\Delta E_m}}{E_m^0} = -\frac{\Delta A}{A_0}\int_{l_1}^{L}\left[\left(\frac{h_m^0}{h_m^{\text{amp}}}\right)^2 - \left(\frac{q_m^0}{q_m^{\text{amp}}}\right)^2\right]\frac{dx}{L}$$

$$= \int_{l_1}^{L}\left(\frac{|\Delta U_m|}{E_m^0} - \frac{|\Delta T_m|}{E_m^0}\right)dx \quad (22)$$

Equation (22) shows that the eigenfrequency shift is related directly to the change in energy for blockages whose radial extent is small enough that the head and flow of each mode for the blocked pipe are approximately equal to the blockage-free case (i.e. h_m and q_m with and without blockage are the same (Fig. 4).

Inserting Eq. (20) into Eq. (22) and carrying out the integration yields (see Appendix 1):

$$\frac{\overline{\Delta w_m}}{w_m^0} = -\frac{\overline{\Delta E_m}}{E_m^0} = \frac{\Delta A}{2L(2m-1)\frac{\pi}{2L}A_0} \times \begin{bmatrix} \sin((2m-1)\pi) \\ -\sin((2m-1)\pi - (2m-1)\pi\eta_2) \end{bmatrix} = \frac{-\Delta A}{(2m-1)\pi A_0}\sin((2m-1)\pi\eta_2) \quad (23)$$

which gives:

$$\frac{\overline{\Delta w_m}}{w_1^0} = -(2m-1)\frac{\overline{\Delta E_m}}{E_m^0} = \frac{(1-\alpha)}{\pi}\sin\left(2\pi(2m-1)\frac{\eta_2}{2}\right) \quad (24)$$

Equation (24) is consistent with the form in Qunli and Fricke (1989) and Duan et al. (2013), and shows the explicit relationship between eigenfrequency shift and change in energy resulting from the extended blockage. It is clear from Eq. (24) that when α tends to 1 (i.e. blockage-free case), both the eigenfrequency shift and the change in energy approach zero for all η_2. In addition, Fig. 5 exhibits the eigenfrequency variation given by Eq. (24) as well as that given by the full dispersion relation (Eq. (2)) for the case of mode $m = 2$. Good quantitative agreement between Eq. (2) and its approximate form (Eq. (24))

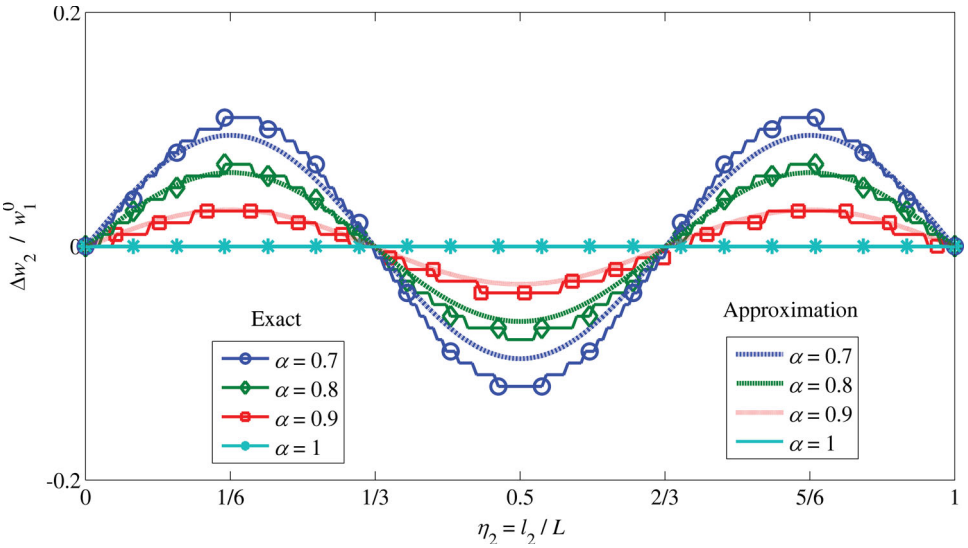

Figure 5 Normalized eigenfrequency variation with length η_2 for $m = 2$: comparison between exact solution (Eq. (2)) and approximate solution (Eq. (24)) (energy approach)

is found for $\alpha \geq 0.7$. There is overall qualitative agreement between these two equations for all α. Although not plotted here, a similar conclusion is found for other m modes. Such agreement supports the application of the principle of action invariance to analyse the eigenfrequency shift induced by a blockage in terms of the change in energy in a pipe due to the presence of blockage.

It could be shown that Eq. (24) is symmetric around $\eta_2 = 0.5$ which agrees with the symmetry feature observed in Fig. 2. This symmetry feature is a special instance of the junction case under consideration, and therefore is not general to all random variation of blockages in a pipe system. More involved and complex blockage in a pipe will be considered in future work.

3.2 *Work of the radiation pressure*

The change in energy of the mth mode, given by Eq. (24), is due to the work done to form the blockage (Schroeder, 1967). This work is performed against the radiation pressure and it is derived below. The term "radiation pressure" is used in acoustic, ocean and costal engineering. It is the difference between the average pressure at a surface moving with the sound displacements (the Lagrangian pressure) and the pressure that would have existed in the fluid of the same mean density at rest (Beyer, 1978). In this paper, the work of radiation pressure refers to the work done to create the blockage. Once the blockage is created, the work of radiation pressure would then refer to the work to hold the blockage still at its location. To relate the change in energy to the work of the radiation pressure (e.g. Beyer, 1978; Borgnis, 1953), multiply Eq. (6) by the complex conjugate of head ($\overline{h_m^0}$) and Eq. (5) by the complex conjugate of the velocity ($\overline{V_m^0}$). Taking the difference gives:

$$\overline{V_m^0}\frac{dh_m^0}{dx} - \overline{h_m^0}\frac{dV_m^0}{dx} = iw_m^0\left(\frac{g\overline{h_m^0}h_m^0}{a^2} - \frac{\overline{V_m^0}V_m^0}{g}\right) \tag{25}$$

Adding $h_m^0\frac{d\overline{V_m^0}}{dx} - h_m^0\frac{d\overline{V_m^0}}{dx}$ to the left hand side of Eq. (25) gives:

$$\frac{d(h_m^0\overline{V_m^0})}{dx} - \left(\overline{h_m^0}\frac{dV_m^0}{dx} + h_m^0\frac{d\overline{V_m^0}}{dx}\right) = iw_m^0\left(\frac{g\overline{h_m^0}h_m^0}{a^2} - \frac{\overline{V_m^0}V_m^0}{g}\right) \tag{26}$$

Note that:

$$\overline{h_m^0}\frac{dV_m^0}{dx} + h_m^0\frac{d\overline{V_m^0}}{dx} = \overline{h_m^0}\frac{dV_m^0}{dx} + \overline{h_m^0\frac{dV_m^0}{dx}} \tag{27}$$

where according to Eq. (6):

$$-\frac{igw_m^0h_m^0\overline{h_m^0}}{a^2} = \overline{h_m^0}\frac{dV_m^0}{dx} \tag{28}$$

Thus, we get:

$$\overline{h_m}\frac{dV_m^0}{dx} + \overline{h_m^0\frac{dV_m^0}{dx}} = -\frac{igw_m^0h_m^0\overline{h_m}}{a^2} + \frac{igw_m^0h_m^0\overline{h_m^0}}{a^2} = 0 \tag{29}$$

and therefore:

$$\frac{d(h_m^0\overline{V_m^0})}{dx} = i\frac{w_m^0}{g}\underbrace{\left(\frac{g^2}{a^2}\overline{h_m^0}h_m^0 - \overline{V_m^0}V_m^0\right)}_{\text{radiation pressure}} \tag{30}$$

The work of the radiation pressure to form the blockage is:

$$\int_{l_1}^{L}\Delta A\frac{\rho}{2}\left(\frac{g^2}{a^2}\overline{h_m^0}h_m^0 - \overline{V_m^0}V_m^0\right)dx = -\frac{ig}{w_m^0}\frac{\rho}{2}\int_{l_1}^{L}\Delta A\frac{d(h_m^0\overline{V_m^0})}{dx}dx \tag{31}$$

Equation (31) shows that:

$$\begin{aligned}&\int_{l_1}^{L}\Delta A\frac{\rho}{2}\left(\frac{g^2}{a^2}\overline{h_m^0}h_m^0 - \overline{V_m^0}V_m^0\right)dx\\ &= -\frac{ig}{w_m^0}\frac{\rho}{2}\int_{l_1}^{L}\Delta A\frac{d(h_m^0\overline{V_m^0})}{dx}dx\\ &= \frac{ig}{w_m^0}\frac{\rho}{2}\Delta A[(h_m^0\overline{V_m^0})_L - (h_m^0\overline{V_m^0})_{l_1}]\end{aligned} \tag{32}$$

Using Eq. (22) gives:

$$\begin{aligned}\frac{\overline{\Delta w_m}}{w_m^0} &= \mathrm{Re}\left[\frac{ig}{E_m^0w_m^0}\frac{\rho}{2}\frac{\Delta A}{A}\int_{l_1}^{L}\frac{d(h_m^0\overline{q_m^0})}{dx}dx\right]\\ &= \xi_m\left[\left(\frac{h_m^0\overline{q_m^0}}{h_m^{\mathrm{amp}}\overline{q_m^{\mathrm{amp}}}}\right)_{l_1} - \left(\frac{h_m^0\overline{q_m^0}}{h_m^{\mathrm{amp}}\overline{q_m^{\mathrm{amp}}}}\right)_L\right]\end{aligned} \tag{33}$$

with:

$$\xi_m = -i\frac{\rho g}{2w_m^0E_m^0}\frac{\Delta A}{A}h_m^{\mathrm{amp}}\overline{q_m^{\mathrm{amp}}} = \frac{a}{w_m^0L}(1-\alpha) \tag{34}$$

and "Re" denotes real part. With comparison with Eq. (22) which relates the change in eigenfrequency to the change in energy within the blocked section, Eq. (33) shows that the eigenfrequency shift depends on the difference between the works done at the blockage boundaries. Therefore, Eq. (33) shows that it is sufficient to only study the work done at the blockage boundary to obtain the eigenfrequency variation which is much simpler approach than studying the change in energy (Eq. (22)). Equation (33) is used in Sections 3.3 and 3.4 to study the shift behaviour.

For the current case of a blockage at the downstream boundary, the work at the valve is always zero, and therefore, Eq. (33) simply becomes:

$$\frac{\overline{\Delta w_m}}{w_m^0} = \xi_m\left(\frac{h_m^0\overline{q_m^0}}{h_m^{\mathrm{amp}}\overline{q_m^{\mathrm{amp}}}}\right)_{l_1} \tag{35}$$

Inserting Eq. (20) into Eq. (35) leads to Eq. (24).

Equation (33) has the freedom to be applied to random variations of cross-sectional area. Equation (33) will be used in future work to study more involved blocked pipe systems.

Table 1 Zero shift location at the first four modes

Mode number	Blockage location
$m = 1$	$\eta_2 = 0, 1$
$m = 2$	$\eta_2 = 0, 1/3, 2/3, 1$
$m = 3$	$\eta_2 = 0, 1/5, 2/5, 3/5, 4/5, 1$
$m = 4$	$\eta_2 = 0, 1/7, 2/7, 3/7, 4/7, 5/7, 6/7, 1$

3.3 *Analysis and discussion of the zero eigenfrequency shift*

This section explains the mechanism of zero shift from different aspects: first analytically; second through energy perspective; third using the work of radiation pressure (Eq. (33)); fourth, and finally, through intuitive and physical perspective. The fourth perspective shows that the system could be seen to be divided into two subsystems (I & II) with fundamental frequencies the same as the whole intact pipe system. Details are given in what follows.

Figure 2 shows there is zero shift for cases shown in Table 1. This result can be generalized for all m by setting Eq. (24) to zero:

$$\begin{aligned} \sin\left(2\pi(2m-1)\frac{\eta_2}{2}\right) = 0 \Rightarrow \pi(2m-1)\eta_2 = (\tau-1)\pi; \\ \tau = 1, 2, 3 \ldots \\ \Rightarrow \eta_2 = \eta_2(m,\tau) \\ = \frac{\tau-1}{(2m-1)} \leq 1;\ \tau \leq 2m \end{aligned} \tag{36}$$

Equation (36) gives the length of the blockage for which the mth mode experiences no shift. Note that the condition that $\tau \leq 2\,m$ is due to the fact that the blockage cannot be longer than the pipe (i.e. $\eta_2 \leq 1$). The values of η_2 where zero shift is obtained from Fig. 2 can be derived by evaluating Eq. (36) for $m = 1, 2, 3$ and 4. For example, evaluating Eq. (36) for $m = 2$ gives $\eta_2(2,1) = 0, \eta_2(2,2) = 1/3$, $\eta_2(2,3) = 2/3$ and $\eta_2(2,4) = 1$. These values correspond to the zero shift locations shown in Fig. 2.

From an energy perspective, Eq. (22) shows that the zero shift of the mth mode occurs when the blockage produces either (i) zero change in the elastic potential energy and the kinetic energy; or (ii) non-zero but equal change in potential and kinetic energy. This is illustrated in Fig. 6 for $m = 2$. It is evident that the change in potential and kinetic energy are non-zero, but equal at $\eta_2 = 1/3$, while the change in both potential and kinetic energy are zero at $\eta_2 = 0, 2/3, 1$ (Fig. 6).

The zero eigenfrequency shift of mode m due to a blockage means that the work done by the radiation pressure to form the blockage is zero (Schroeder, 1967). According to Eq. (33) this work is zero when either the pressure or velocity at the edge of the blockage is zero. When the blockage extends from the valve to $x = 2L/3$, the pressure of mode $m = 2$ is zero at $x = 2L/3$ (Fig. 7). Therefore, the work of the radiation pressure is zero, implying the change in energy of mode $m = 2$ is zero and, thus, the eigenfrequency shift is zero. When the blockage extends from the valve to $x = L/3$, the velocity of mode $m = 2$ is zero at $x = L/3$ (Fig. 7). Therefore, the work of the radiation pressure is zero, implying the change in energy of mode $m = 2$ is zero and, thus, the eigenfrequency shift is zero. In general, the eigenfrequency shift of mode m is zero when the values of $h_m V_m$ of this mode at either end of the blockage are equal.

Physically, when the blockage extends from the downstream end to the pressure node ($\eta_2 = 2/3$, case (a) in Fig. 7), the pipe system for this mode $m = 2$ is effectively divided into two pipe subsystems. Subsystem I is a RPV with a pipe length equal to the blockage length $l_2 = L/3$. Subsystem II is a reservoir-pipe-reservoir with a pipe length equal to $l_1 = L - l_2 = 2L/3$. The wavelengths of the natural modes of subsystem I are $\lambda_n = 4l_2/(2n-1) = 4L/3(2n-1)$ for $n = 1, 2 \ldots$. Therefore, the wavelength of the fundamental ($n = 1$) mode is $\lambda_1 = 4l_2$ which explains the quarter wave in subsystem I (Fig. 8, case

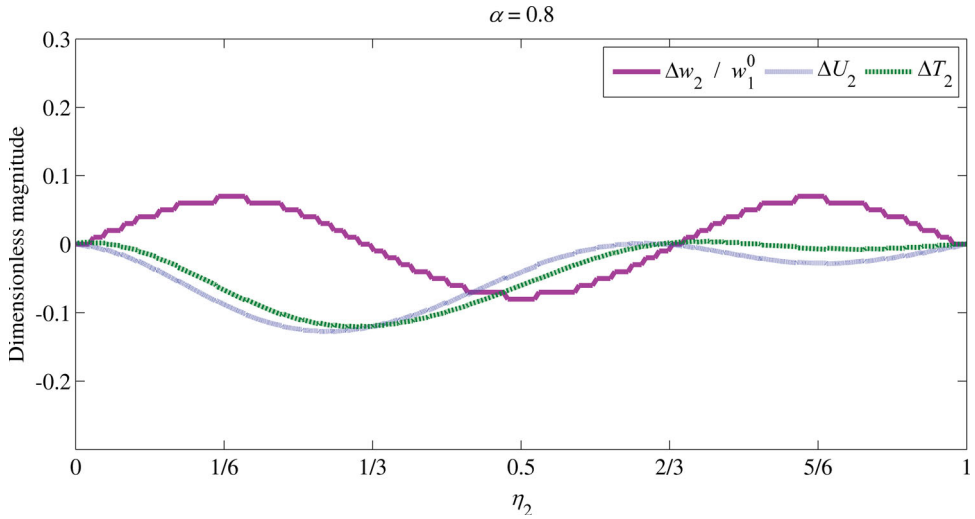

Figure 6 Variation with η_2 of total change in potential and kinetic energy in the pipe with blockage along with the eigenfrequency shift at mode $m = 2$ and $\alpha = 0.8$

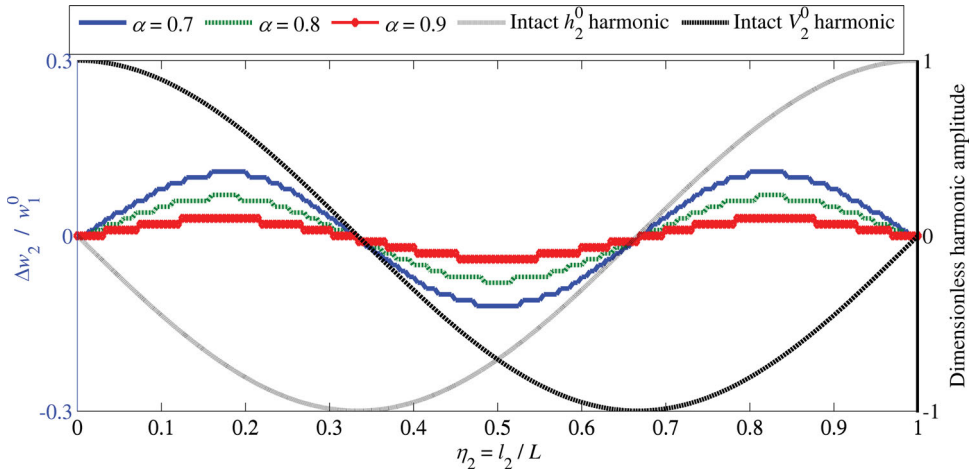

Figure 7 Eigenfrequency shift variation at mode $m = 2$ for different α values along with the intact pressure harmonic

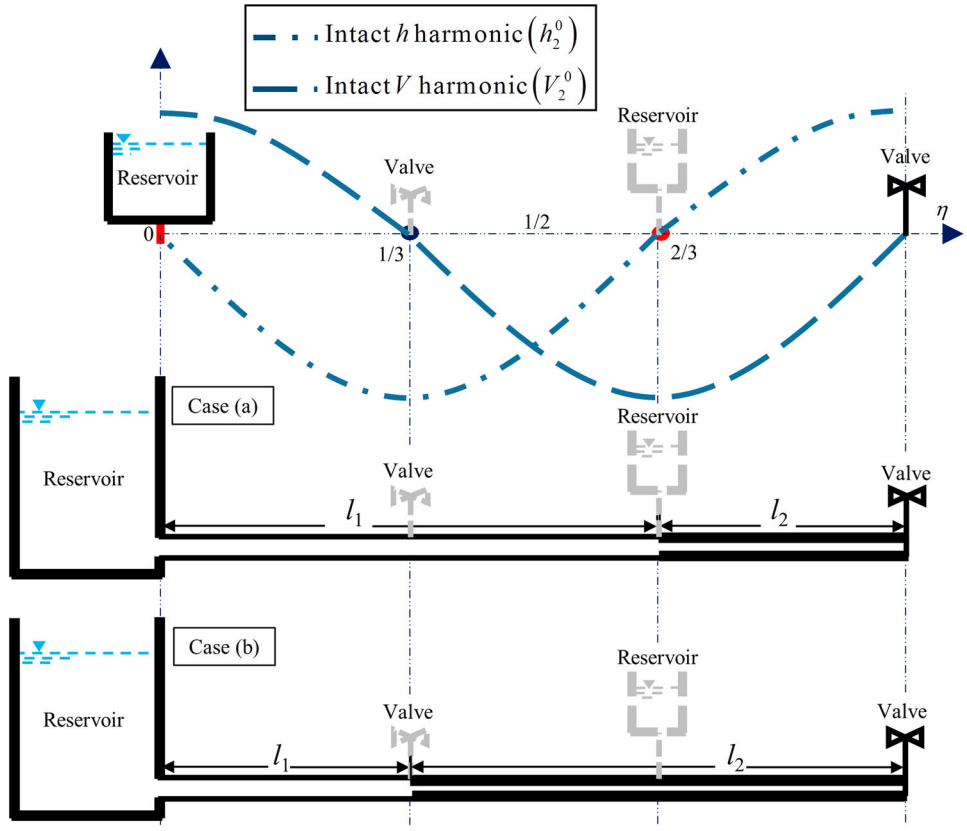

Figure 8 Sketch depicting how the harmonic at mode $m = 2$ is subdivided into single subharmonics. Case (a) and case (b) correspond to the zero shift cases where $\eta_2 = 1/3$ and $\eta_2 = 2/3$, respectively

(a)). The wavelengths of the natural modes of subsystem II are $\lambda_n = 2l_2/n = 4L/3n$ for $n = 1, 2 \ldots$. Therefore, the wavelength of the fundamental ($n = 1$) mode is $\lambda_1 = 2l_2$, which explains the half wave in subsystem II (Fig. 9, case (a)). That is, mode $m = 2$ of the whole pipe system is made up of the two fundamental modes of subsystems I and II. The same reasoning can be used to explain the subsystems in Fig. 8, case (b), as well as the zero shifts that occur for other modes m.

3.4 *Analysis and discussion of the positive and negative eigenfrequency shift*

Figure 2 shows that the first four modes experience positive shift and negative shift for blockage locations as given in Table 2. These observations are corroborated by Eq. (24).

Equation (22) shows that a positive eigenfrequency shift in mode m occurs when the presence of the blockage results in a

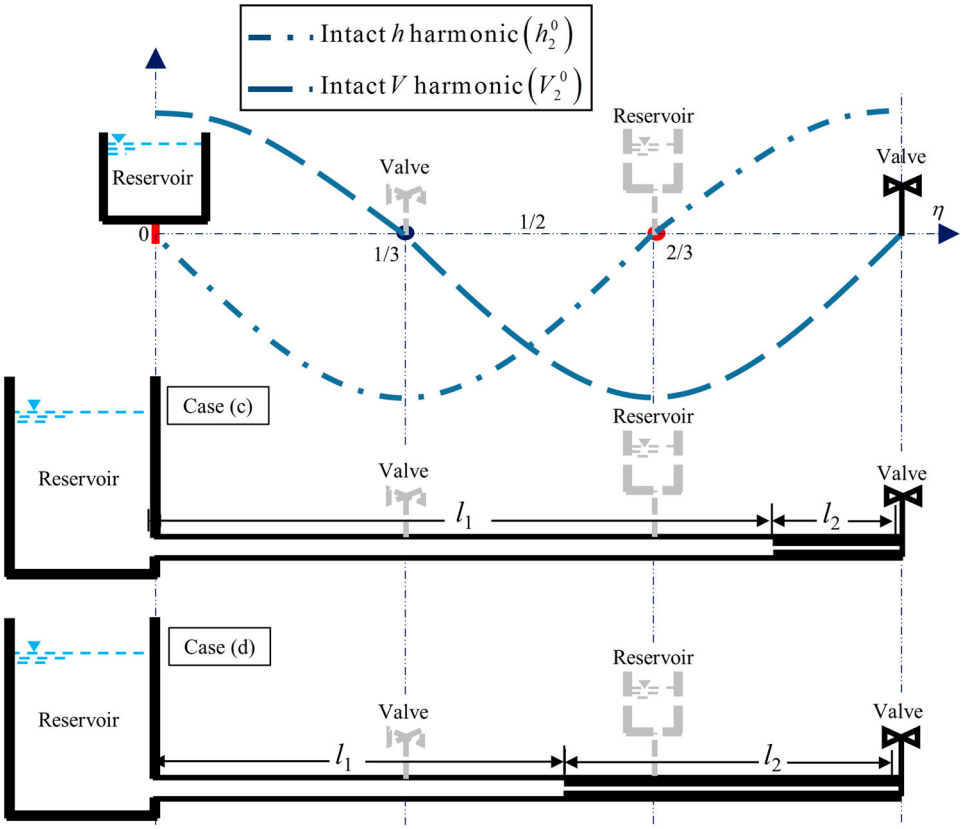

Figure 9 Sketches of the junction system for two shift cases: case (c) leads to positive shift ($\eta_2 = 1/6$) and case (d) leads to negative shift ($\eta_2 = 5/12$)

Table 2 Blockage locations that lead to positive and negative shift at the first four modes

Mode number	Blockage location for positive shift	Blockage location for negative shift
$m = 1$	η_2 in]0 , 1[	No negative shift
$m = 2$	η_2 in]0 , 1/3[∪]2/3 , 1[	η_2 in]1/3 , 2/3[
$m = 3$	η_2 in]0 , 1/5[∪]2/5 , 3/5[∪]4/5 , 1[	η_2 in]1/5 , 2/5[∪]3/5 , 4/5[
$m = 4$	η_2 in]0 , 1/7[∪]2/7, 3/7[∪]4/7 , 5/7[∪]6/7 , 1[	η_2 in]1/7 , 2/7[∪]3/7 , 4/7[∪]5/7 , 6/7[

net negative change in the total energy of this mode. This in turn occurs when the change in elastic potential energy is larger than the change in kinetic energy (see right hand side of Eq. (22)). Conversely, Eq. (22) shows that a negative eigenfrequency shift in mode m occurs when the presence of the blockage results in a net positive change in the total energy of this mode. This, in turn, occurs when the change in elastic potential energy is less than the change in kinetic energy (see right hand side of Eq. (22)). This is illustrated in Fig. 6 for the case of $m = 2$. In particular, Fig. 6 shows that the change in elastic potential energy is larger than the change in kinetic energy of mode $m = 2$ for η_2 in]0, L/3[∪]2L/3, L[which is the region where there is a positive eigenfrequency shift of mode $m = 2$ (Fig. 2). In addition, Fig. 6 shows that change in elastic potential energy is less than the change in kinetic energy of mode $m = 2$ for $\eta_2$in]L/3, 2L/3[which is the region where there is negative eigenfrequency shift of mode $m = 2$ (Fig. 2).

To further investigate the eigenfrequency shift in mode $m = 2$, Fig. 9 shows two cases for which the shift is positive (case (c)) and negative (case (d)). The pressure head and velocity harmonics corresponding to case (c) and case (d) are given in Fig. 10a and 10b, respectively. It is clear from Fig. 10a that mode $m = 2$ has a positive h and a negative V at $x = 5L/6$. Therefore, $hV\Delta A$ of this mode is negative at $x = 5L/6$, implying that the work of the radiation pressure (Eq. (31)) and the change in energy for a blockage that extends from the valve to $x = 2L/3$ are negative. This explains why mode $m = 2$ experiences a negative shift in this case (Fig. 2). Figure 10b shows that mode $m = 2$ has negative h and V at $x = 7L/12$. Therefore, $hV\Delta A$ of this mode is positive at $x = 7L/12$ implying that the work of the radiation pressure (Eq. (31)) and the change in energy for a blockage that extends from the valve to $x = 7L/12$ are positive. This explains why mode $m = 2$ experiences a positive shift in this case (Fig. 2). In fact, $hV\Delta A$ of the mth mode varies assin[$(2m-1)\,\pi\,\eta_2$] ; thus, there is (i) a positive shift when the argument of the sine function varies is in the range $]2\mu\pi, (2\mu+1)\pi[$ where μ is an integer counting number; and (ii) a negative shift otherwise. In general, a given mode m experiences negative eigenfrequency shift when the work of the radiation pressure due to the formation of the blockage is positive and experiences a positive eigenfrequency shift when the work of the radiation pressure due to the formation of the

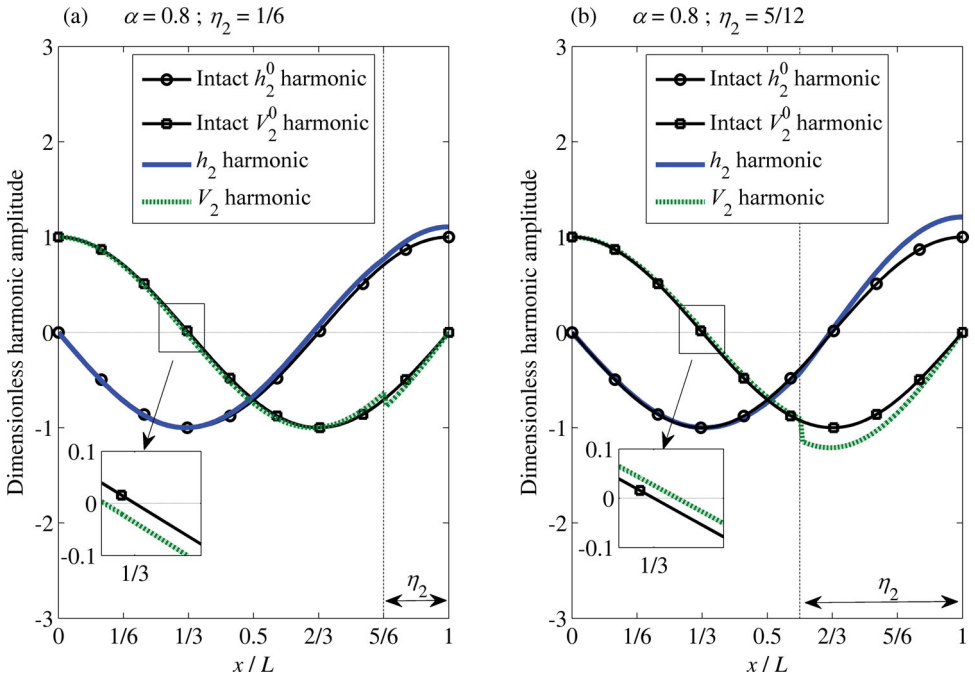

Figure 10 Dimensionless pressure and velocity harmonics when $m = 2$ and $\alpha = 0.4$: $(a)\eta_2 = 1/6$; leads to positive shift $(b)\eta_2 = 5/12$ leads to negative shift. The black square boxes are sketch of the cross sectional area reduction

blockage is negative. It is noted that a positive eigenfrequency shift is sometimes referred to as *length shortening* and a negative eigenfrequency shift as *length extending* (e.g. Qunli and Fricke 1989).

The maximum eigenfrequency shift position corresponds to the length of the blockage at which the change in energy is an extremum. Mathematically, this occurs when the derivative of Eq. (24) is zero; that is:

$$\begin{aligned}\cos\left(2\pi(2m-1)\frac{\eta_2}{2}\right) = 0 \Rightarrow 2\pi(2m-1)\frac{\eta_2}{2} \\ = (2n-1)\frac{\pi}{2}; n = 1,2,3 \\ \Rightarrow \eta_2 = \eta_2(m,n) = \frac{(2n-1)}{2(2m-1)} \leq 1; \quad n \leq 2m-1\end{aligned} \tag{37}$$

For example, consider the case of $m = 2$. The condition, $n \leq 2m-1 = 3$ gives $n = 1$, 2 and 3. Therefore, there are three maxima at 1/6, 1/2 and 5/6 (Fig. 5). These maxima correspond to $h_m V_m \ \Delta A$, which varies as $\sin[\,(2m-1)\,\pi\eta_2]$, having the largest magnitude (i.e. where the work of the radiation pressure is extremum).

4 Analysis and discussion of frequency-blockage interaction for blockage with large radial protrusion (i.e. α near 0)

The previous section is devoted to blockage with small radial protrusion. In this section, a blockage with large radial protrusion (referred to as severe blockage in this paper) is investigated.

For a severe blockage (i.e. α tends to 0), Eq. (1) reduces to:

$$\cos(kl_1)\cos(kl_2) = 0 \tag{38}$$

which implies:

$$\cos(kl_1) = 0 \Rightarrow \frac{w_m^{s_1}}{w_1^0} = \frac{(2m-1)}{\eta_1}; \quad m = 1,2,3\ldots \tag{39}$$

or

$$\cos(kl_2) = 0 \Rightarrow \frac{w_m^{s_2}}{w_1^0} = \frac{(2m-1)}{\eta_2}; \quad m = 1,2,3\ldots \tag{40}$$

where w_1^0 is the first eigenfrequency of the intact pipe case and $w_m^{s_1}$ and $w_m^{s_2}$ are the mth eigenfrequencies for the case of severe blockage. Effectively, the severe blockage decouples the pipe system responses into two independent subsystems. Subsystem 1 consists of the pipe with length l_1 bounded by the upstream reservoir and the blockage. The blockage, being severe, would act in a manner similar to a valve. That is, a severe blockage imposes a large impedance on the flow as a valve would. Therefore, the response of subsystem 1 is equivalent to a RPV system. In fact, the resonant frequencies given by Eq. (39) are for a RPV system, where the pipe has a length l_1. It is for this reason that a superscript "s_1" is used in Eq. (39). Subsystem 2 consists of another RPV system in which the narrow blockage opening functions as a small diameter pipe of length l_2, while the much larger pipe diameter of lengths l_1 acts as a reservoir. Indeed, the resonant frequencies given by Eq. (40) are for a RPV system, where the pipe has a length l_2.

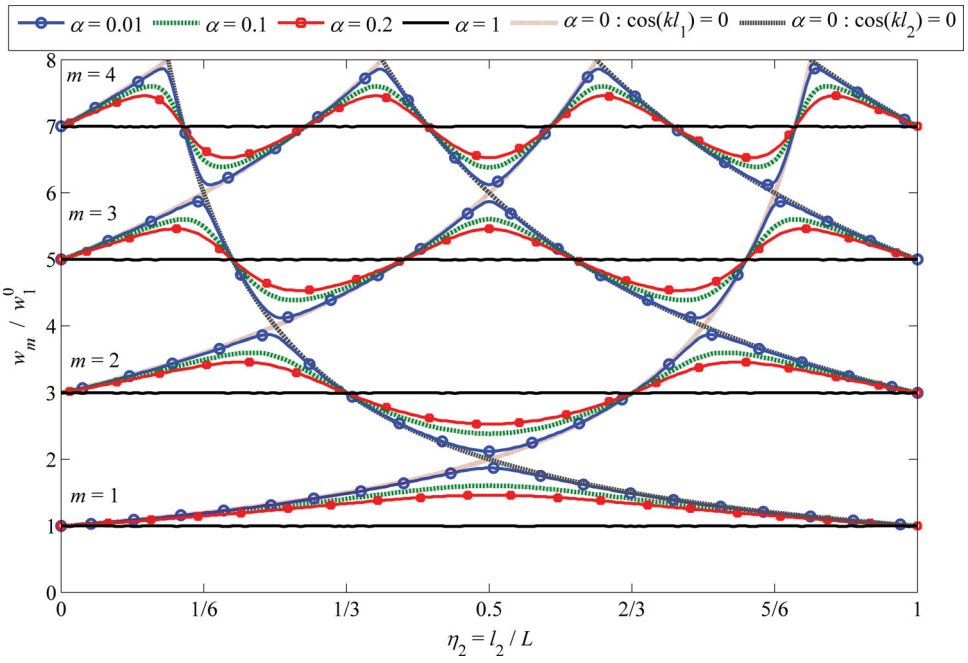

Figure 11 Dimensionless eigenfrequency variation with length η_2 of the first four modes for different α along with the asymptotic solution from Eqs (39) and (40)

The decoupling of the pipe system into two subsystems can be understood from an energy perspective. The ratio of reflected to incident energy at the interface between the blocked and unblocked pipe sections is (Lighthill, 1978) $(Z_1-Z_2)^2/(Z_1+Z_2)^2 = (\alpha-1)^2/(\alpha+1)^2$, where $Z_1 = \rho a/A_0$ is the impedance of the unblocked pipe section and $Z_2 = \rho a/A_2$ is the impedance of the pipe section that has the severe blockage. The ratio of the transmitted to incident energy at the interface between the blocked and unblocked pipe sections is $4Z_1Z_2/(Z_1+Z_2)^2 = 4\alpha/(\alpha+1)^2$. Clearly, as α tends to 0, the reflection coefficient approaches 1 and the transmission coefficient approaches zero. Therefore, a wave that is generated in subsystem 1 is largely trapped in this subsystem. Conversely, a wave that is generated in subsystem 2 is largely trapped in this subsystem. It is in this sense that the decoupling should be understood.

The eigenfrequencies of the whole system are the union of the eigenfrequencies of subsystems 1 and 2. That is, $w_m = \{(2m-1)\ a\pi/(2l_1)\} \cup \{(2m-1)\ a\pi/(2l_2)\}$, where $\cup$ is the union operator. It is clear that if the blockage length l_2 is much smaller than l_1, then the low frequencies are governed by subsystem 1 and vice versa. To see this, consider Fig. 11. The fundamental frequencies of subsystem 1 ($\cos(kl_1) = 0$) and subsystem 2 ($\cos(kl_2) = 0$) are plotted for $m = 1$, 2, 3 and 4. It can be seen that w_1, w_2, w_3 and w_4 are governed by subsystem 2 for a short (i.e.η_2 close to 0) blockage and by subsystem 1 for a long (i.e.η_2 close to 1) blockage. For example, using Eq. (39), the first four dimensionless eigenfrequencies for subsystem 1 for $\eta_2 = 1/3$ are 3/2, 9/2, 15/2 and 21/2. In addition, using Eq. (40), the first four dimensionless eigenfrequencies for subsystem 2 for $\eta_2 = 1/3$ are 3, 9, 15 and 21. The union of these eigenfrequencies is $\{3/2, 9/2, 15/2, 21/2\} \cup \{3, 9, 15, 21\} = \{3/2, 3, 9/2, 15/2, 9, 21/2, 15, 21\}$. Therefore, the first four dimensionless resonant frequencies for the overall system are {3/2, 3, 9/2, 15/2} which agree with values that can be read from Fig. 11 when $\eta_2 = 1/3$. Note that the first, third and fourth of these frequencies are the first three resonant frequencies of subsystem 1 and the second is the eigenfrequency of subsystem 2. In the preceding eigenfrequency sets, the four fundamental frequencies of the overall system are determined manually by calculating the four fundamental frequencies of each subsystem and then sorting them from lowest to largest value. An algorithm that automates this sorting process is given in Appendix 2.

Equation (B4) (see Appendix 2) gives the different asymptotic branches at a given mode m as η_2 varies, and as observed from Fig. 11, these branches define the solution domain of the eigenfrequency shift variations for $0 \leq \alpha \leq 1$.

5 Analysis and discussion of frequency-blockage interaction for blockage with moderate radial protrusion

The last two sections focused on blockages with small radial protrusion (α near 1) and blockages with large radial protrusion (α near 0). It is found that the small blockage assumption is accurate for $\alpha \geq 0.7$(Fig. 5). In addition, the large blockage assumption is valid for $\alpha < 0.7$ provided that the values of the frequencies of subsystem 1 (Eq. ((39)) and subsystem 2 (Eq. (40)) are not equal or close to each other (Fig. 11). This section focuses on the case $\alpha < 0.7$for systems where the frequencies of subsystem 1 (Eq. (39)) and subsystem 2 (Eq. (40)) are equal

or near each other. In this case, the waves in subsystem 1 act as forcing functions to subsystem 2, where the forcing frequency is equal or close to the eigenfrequency of subsystem 2. Similarly, the waves in subsystem 2 act as a forcing function to subsystem 1, where the forcing frequency is equal or close to the eigenfrequency of subsystem 1. That is, both subsystems are driven at or near resonance. Therefore, although the ratio of transmitted to incident energy on the interface between the blocked and unblocked pipe sections of each incoming wave is of the order of $4\alpha/(\alpha+1)^2$ (i.e. small), the fact that each of the two subsystems is driven near its resonance frequency means that the transmitted energy accumulates with time and forces the overall system to behave more as a coupled rather than an uncoupled system.

To first order, the wavenumbers and eigenfrequencies of the coupled system are those of the uncoupled system plus a perturbation (i.e. $k_m = k_m^s + \delta k_m$ and $w_m = w_m^s + \delta w_m$). Therefore, Eq. (1) gives: $\delta k_m = \pm\sqrt{\alpha/(l_1 l_2)}$, which gives $\delta w_m = \pm a\sqrt{\alpha/(l_1 l_2)}$. To illustrate this, consider the case $\alpha = 0.2, m = 1$, $l_1 = L/2 = l_2$. Then, $\delta w_1/w_1^0 = \pm(\alpha/l_1 l_2)^{1/2}/(\pi/2L) = \pm(\alpha/L/2L/2)^{1/2}/(\pi/2L) = \pm(4/\pi)(\alpha)^{1/2} = \pm 0.569$, which is in good agreement with the deviations that can be read from Fig. 11. Note that $\delta w_m = \pm a\sqrt{\alpha/(l_1 l_2)}$ is independent of m, which agrees with Fig. 2.

It is noted from Fig. 11 that the zero shift is independent of α. This result can be explained from Eq. (1). In particular, for any $\alpha \neq 1$, Eq. (1) gives the intact pipe frequencies whenever the blockage length is such that either $\sin(kl_1) = 0$ or $\sin(kl_2) = 0$.

Figure 2 shows that the position of the maximum shift changes as a function of α except when the blockage length is half of the pipe length (i.e. $\eta_2 = 0.5$). An expression for the maximum eigenfrequency shift and the location η_2 at which it occurs can be obtained from Eq. (2) as follows:

$$\cos(kL) + \frac{1-\alpha}{1+\alpha}\cos(kL - 2kl_2) = 0 \tag{41}$$

where the second term on the left hand side of Eq. (41) is what causes the shift in frequency. The maximum shift occurs when that term is maximum, which gives:

$$\begin{aligned} \sin(kL - 2kl_2) = 0 \Rightarrow k_m^{\max}L - 2k_m^{\max}l_2 \\ = (n-1)\pi; \quad n = 1,2,3\ldots \\ \Rightarrow \cos(k_m^{\max}L - 2k_m^{\max}l_2) = (-1)^{(n-1)} \end{aligned} \tag{42}$$

where $k_m^{\max} = w_m^{\max}/a$ is the wavenumber corresponding to the maximum mth eigenfrequency ($w_m^{\max}$) magnitude at a given α. Inserting Eq. (42) into Eq. (41) yields:

$$\begin{aligned} \Rightarrow k_m^{\max}L = \operatorname{acos}\left[(-1)^{n+m-1}\left(\frac{1-\alpha}{1+\alpha}\right)\right] \\ + (m-1)\pi; \quad m = 1,2,3\ldots \end{aligned} \tag{43}$$

which gives:

$$\begin{cases} \dfrac{\Delta w_m^{\max}(m,\alpha,n)}{w_1^0} = \dfrac{w_m^{\max} - w_m^0}{w_1^0} \\ = \dfrac{2}{\pi}\operatorname{acos}\left[(-1)^{n+m}\left(\frac{1-\alpha}{1+\alpha}\right)\right] - 1 \\ \text{where } n \equiv n-1 = 1,2,3\ldots \text{ and } m = 1,2,3\ldots \end{cases} \tag{44}$$

where $\Delta w_m^{\max}(m,\alpha,n)$ is the maximum shift at a given mode m, a given $\alpha$and a given positive or negative shift region n (between two successive zero shift locations (Fig. 2 and Eq. (36)). In Eq. (44), $n-1$ was replaced by n so that the first ($n = 1$) shift magnitude is positive. For example, the first shift region ($n = 1$) as η_2 increases in Fig. 2 is located at $\eta_2(2,1) = 0 \le \eta_2 \le \eta_2(2,2) = 1/3$ (Fig. 2 and Eq. (36)). Thus, at mode $m = 2$, $\alpha = 0.2$ and $n = 1$, Eq. (42) shows that the magnitude of the eigenfrequency shift is $\Delta w_m^{\max}(2,0.2,1)/w_1^0 = 0.4646$ which agrees with Fig. 11.

The location corresponding to each maximum shift is obtained by inserting Eq. (43) into Eq. (42) which leads to:

$$\Rightarrow \begin{cases} \eta_2 = \eta_2(m,\alpha,n) = \frac{1}{2}\left[1 - \frac{(m-n)\pi}{\operatorname{acos}((-1)^{2m-n}\frac{1-\alpha}{1+\alpha}) + m\pi}\right]; \\ \text{where } n-1 \equiv (m-n) \le 2m \text{ and } 0 \le \eta_2 \le 1 \end{cases} \tag{45}$$

For example, at mode $m = 2$, $\alpha = 0.2$ and $n = 1$, Eq. (45) shows that the position of the maximum shift is $\eta_2(2,0.2,1) = 0.2114$, which agrees with Fig. 11.

6 Conclusions

The eigenfrequency shift due to variation in the cross sectional area of a conduit is investigated with the primary goal being to understand and describe the mechanisms that cause the eigenfrequency shift caused by a conduit blockage. The theoretical model considered consists of a RPV containing a single blockage that may have different radial and longitudinal extent. The key findings are:

(1). The assumption of small blockage is applicable when the blockage occupies 30% of the pipe's area or less. The assumption of severe blockage is applicable when the blockage occupies 30% of the pipe's area or more provided that the eigenfrequencies of waves in the blockage zone and waves outside the blockage zone are not close or equal.

(2). A small blockage reduces the elastic potential energy, but increases the kinetic energy of all modes. In addition, w_m E_m is conserved, implying $\Delta w_m/w_m = -\Delta E_m/E_m$ for all modes m, and the change in energy is found to equal the work of the radiation pressure during the formation of the blockage. The test cases confirm that (i) a blockage that causes an increase in total energy of a mode m would produce a negative shift of the eigenfrequency of this mode;

(ii) a blockage that causes a decrease in total energy of a mode m would produce a positive shift of the frequency of this mode; and (iii) blockage that causes a zero change in total energy of a mode m would produce no shift of the frequency of this mode.

(3). A severe blockage decouples the pipe system into two independent subsystems. The ratio of the reflected to incident energy at the interface between the blocked and unblocked pipe sections is about 1 while the transmission coefficient is about 0. The eigenfrequencies of the overall system are given by the union of the eigenfrequencies of the two decoupled systems.

(4). The decoupling by a severe blockage is lost when the eigenfrequencies of the two subsystems are close or equal to each other. When this happens, waves in the blockage act as forcing functions that drive the rest of the pipe system at or near resonance. Similarly, waves outside the blockage are forcing functions that drive the waves within the blockage at or near resonance. The fact that both subsystems are driving one another at or near resonance is what brings about the coupling even for a very severe blockage. In this case, perturbation theory is found to provide a simple and explicit relationship between the frequency shift and the properties of the blockage.

(5). The methodology presented in this paper can be extended to more general problems. In fact, the authors have already embarked on extending the work to a single pipe but with more realistic blockage, and the results will be reported in future publications.

Acknowledgements

The authors thank Dr D.A. McInnis for the technical and editorial suggestions.

Funding

This study is supported by the Hong Kong Research Grant Council, (projects 612712 & 612713 & T21-602/15R) and by the Postgraduate Studentship.

Appendix

Appendix 1: Governing equations

A.1 *Intact pipe case*

The continuity and momentum equations of an inviscid flow in a single intact pipe case are given by (Chaudhry, 2014):

$$\begin{cases} \dfrac{\partial H}{\partial t} + \dfrac{a^2}{gA_0}\dfrac{\partial Q}{\partial x} = 0 \\ \dfrac{\partial Q}{\partial t} + gA_0\dfrac{\partial H}{\partial x} = 0 \end{cases} \tag{A1}$$

where Q is the instantaneous flow discharge, H is the instantaneous pressure head, g is the acceleration due to gravity, A_0 is the cross-sectional area, a is the acoustic wave speed, x is the distance along the pipe line and t is the time. In steady-oscillatory flow, Q and H could be divided into steady and unsteady parts as follows:

$$\begin{cases} Q = \overline{Q} + q \\ H = \overline{H} + h \end{cases} \tag{A2}$$

where $\overline{Q}$ and $\overline{H}$ are the mean discharge and pressure head, respectively, and q and h are the unsteady discharge and pressure head parts. In what follow, q and h will be referred simply as discharge (flow rate) and pressure head, respectively. Substituting Eq. (A2) into Eq. (A1) gives:

$$\begin{cases} \dfrac{\partial h}{\partial t} + \dfrac{a^2}{gA_0}\dfrac{\partial q}{\partial x} = 0 \\ \dfrac{\partial q}{\partial t} + gA_0\dfrac{\partial h}{\partial x} = 0 \end{cases} \tag{A3}$$

Differentiating the continuity equation with t and the momentum equation with x, Eq. (A3) leads to the following wave equation:

$$\frac{\partial^2 h}{\partial t^2} - a^2\frac{\partial^2 h}{\partial x^2} = 0 \tag{A4}$$

Assuming that q and h are harmonics in time, the solution to Eq. (A4) is:

$$h = [C_1\exp(-ikx) + C_2\exp(ikx)]\exp(iwt) \tag{A5}$$

where $k = w/a$ is the wavenumber with w being the angular frequency and a is the acoustic wave speed in water, C_1 and C_2 are complex constants that depend on the BCs, and $i = \sqrt{-1}$. The pressure head and discharge solution for an intact symmetric pipe system such as valve-pipe-valve and for an anti-symmetric pipe system such as RPV are governed by (Chaudhry, 2014):

$$\begin{cases} h(x,k) = 2C\cos(kx) = h^{\text{amp}}\cos(kx) \\ q(x,k) = -2i\frac{g}{a}A_0C\sin(kx) = q^{\text{amp}}\cos(kx) \end{cases} \tag{A6}$$

and

$$\begin{cases} h(x,k) = 2iC\sin(kx) = h^{\text{amp}}\sin(kx) \\ q(x,k) = -2\frac{g}{a}A_0C\cos(kx) = q^{\text{amp}}\cos(kx) \end{cases} \tag{A7}$$

where h and $q = A_0V$ are the pressure head and flow discharge, respectively, with V the unsteady flow velocity; h^{amp} and q^{amp} are the amplitudes of maximum pressure head and flow discharge, respectively; C is a complex constant of integration; x is the distance along the pipe line from downstream boundary to the upstream boundary. The dispersion relationships that governs the natural resonant frequencies (eigenfrequencies) for

intact valve-pipe-valve and RPV systems can be obtained by imposing the velocity to be zero at $x = L$ (at the valve) as follows:

$$\text{Valve - Pipe - Valve} : \sin(kL) = 0 \Leftrightarrow w_m^0 = ak_m^0 = 2\pi\left((2m)\frac{a}{4L}\right); \quad m = 1, 2, 3\ldots \tag{A8}$$

and

$$\text{Reservoir - Pipe - Valve} : \cos(kL) = 0 \Leftrightarrow w_m^0 = ak_m^0 = 2\pi\left[(2m-1)\frac{a}{4L}\right]; \quad m = 1, 2, 3\ldots \tag{A9}$$

where w_m^0 and k_m^0 are the mth eigenfrequency and wavenumber, respectively; the superscript "0" refers to intact pipe, "m" is the mode number and L is the total length of an intact pipe. Inserting the mth eigenfrequency in the pressure head and flow velocity solution gives the mth mode solution. In linear wave theory, the summation of all the mode solutions gives the overall solution of the pressure and flow velocity as follows:

$$\begin{cases} h = \sum_m h_m \\ q = \sum_m q_m \end{cases} \tag{A10}$$

The mode solution in pipe system depends on the BCs where for example Eq. (A8) gives the even modes and Eq. (A9) gives the odd modes. These mode solutions are also often referred as standing waves or harmonics. The pressure head and flow harmonics are balanced in such a way that as the pressure varies, the elastic potential energy is being transformed into kinetic energy. The relationship between the change in pressure head (Δh) and flow velocity (ΔV) could be obtained from the momentum equation as follows:

$$\Delta h = \pm\frac{a}{g}\Delta V \tag{A11}$$

which corresponds to the Joukowsky relationship in water hammer theory (Ghidaoui, 2004).

A.2 *Junction pipe case*

The transfer matrix method (Chaudhry, 2014) can be used to determine q and h at any location $x \geq l_1$ in the junction pipe system (Fig. 1) as follows:

$$\begin{pmatrix} q(x,k_m) \\ h(x,k_m) \end{pmatrix} = \begin{bmatrix} \cos(k_m(x-l_1)) & -i\frac{gA_2}{a}\sin(k_m(x-l_1)) \\ -i\frac{a}{gA_2}\sin(k_m(x-l_1)) & \cos(k_m(x-l_1)) \end{bmatrix} \times \begin{bmatrix} 1 & 0 \\ 0 & 1 \end{bmatrix} \times \begin{bmatrix} \cos(k_m l_1) & -i\frac{gA_0}{a}\sin(k_m l_1) \\ -i\frac{a}{gA_0}\sin(k_m l_1) & \cos(k_m l_1) \end{bmatrix} \times \begin{pmatrix} q(0,k_m) \\ h(0,k_m) \end{pmatrix}; \quad \text{if } x \geq l_1 \tag{A12}$$

where m represents the mth natural harmonic mode and k_m is the mth wavenumber. Equation (A12) can be written as:

$$\begin{pmatrix} q(x,k_m) \\ h(x,k_m) \end{pmatrix} = \begin{bmatrix} U_{11} & U_{12} \\ U_{21} & U_{22} \end{bmatrix} \begin{pmatrix} q(0,k_m) \\ h(0,k_m) \end{pmatrix} \tag{A13}$$

where U_{11}, U_{12}, U_{21} and U_{22} can be determined from the matrix multiplication in Eq. (A12). The pressure head and discharge at the reservoir are given by:

$$\begin{cases} h(0,k_m) = 0 \\ q(0,k_m) = -2\frac{g}{a}A_0 C = q_m^{\text{amp}} = i\frac{g}{a}A_0 h_m^{\text{amp}} \end{cases} \tag{A14}$$

where q_m^{amp} and h_m^{amp} are the maximum flow and pressure head which are complex constant, respectively; C is a complex constant of integration. Using Eq. (A14), Eq. (A13) yields:

$$\begin{aligned} q(x,k_m) &= U_{11} q_m^{\text{amp}} \\ h(x,k_m) &= U_{21} q_m^{\text{amp}} \end{aligned} \tag{A15}$$

Obtaining U_{11} and U_{21} from Eq. (A12) leads to:

$$\Rightarrow \begin{cases} \overline{q_m}(x,k_m) = \dfrac{q_m(x,k)}{q_m^{\text{amp}}} = \begin{bmatrix} \cos(k_m(x-l_1))\cos(k_m l_1) \\ -\alpha\sin(k_m(x-l_1))\sin(k_m l_1) \end{bmatrix} \\ \overline{h_m}(x,k_m) = \dfrac{h_m(x,k)}{h_m^{\text{amp}}} = \dfrac{1}{\alpha}\begin{bmatrix} \sin(k_m(x-l_1))\cos(k_m l_1) \\ +\alpha\cos(k_m(x-l_1))\sin(k_m l_1) \end{bmatrix} \end{cases} \tag{A16}$$

where $\alpha = A_2/A_0$; $\overline{q}$ and $\overline{h}$ are the dimensionless discharge and pressure head, respectively.

The normalized kinetic energy ($\overline{T}_m$) and elastic potential energy ($\overline{U}_m$) at a given location $x \geq l_1$ can be obtained from Eq. (A16) as follows:

$$\begin{cases} \overline{T}_m = \dfrac{T_m}{(\rho/2A_0)(q_m^{\text{amp}})^2} = \dfrac{(\rho/2A_2)q_m^2}{(\rho/2A_0)(q_m^{\text{amp}})^2} \\ = \dfrac{1}{\alpha}\begin{bmatrix} \cos(k_m(x-l_1))\cos(k_m l_1) \\ -\alpha\sin(k_m(x-l_1))\sin(k_m l_1) \end{bmatrix}^2 \\ \overline{U}_m = \dfrac{U_m}{(\rho/2A_0)(q_m^{\text{amp}})^2} = \dfrac{(\rho/2)A_2(g/a)^2 h_m^2}{(\rho/2A_0)(q_m^{\text{amp}})^2} \\ = \dfrac{1}{\alpha}\begin{bmatrix} \sin(k_m(x-l_1))\cos(k_m l_1) \\ +\alpha\cos(k_m(x-l_1))\sin(k_m l_1) \end{bmatrix}^2 \end{cases} \tag{A17}$$

where $k_m = w_m/a$ is the mth wavenumber, w_m is the mth eigenfrequency (natural resonant frequency of the system) with the subscript "m" refers to the mth resonant mode. At the valve where $x = L$, the flow and the kinetic energy are zero, and

therefore, Eq. (A17) gives:

$$\begin{aligned} &\cos(k_m l_2)\cos(k_m l_1) - \alpha \sin(k_m l_2)\sin(k_m l_1) = 0 \\ &\Leftrightarrow \cos(k_m L) + (1-\alpha)\sin(k_m l_2)\sin(k_m l_1) = 0 \end{aligned} \tag{A18}$$

which is the dispersion relation. Equation (A18) could be obtained from the dispersion relationship derived in Duan et al. (2012) under the special case where the blockage is located at the downstream of the pipe.

B Appendix 2: Eigenfrequency solution for uncoupled subsystems

In order to automate this sorting process, Eq. (2) is considered:

$$-1 \le \underbrace{\cos(kL) = -\sin(kl_1)\sin(kl_2)}_{\text{Eq. } 3(\alpha=0)} \le 1 \tag{B1}$$

which gives:

$$2(m-1) \le \frac{w_m^s}{w_1^0} \le 2m; \quad m = 1, 2, 3 \ldots \tag{B2}$$

where w_m^s is the mth eigenfrequency of the whole junction system for the case of very deep (severe) cross sectional area variation (α tends to 0). Imposing the condition in Eq. (B2) on Eqs (39) and (40) gives:

$$\frac{w_m}{w_1^0} = \begin{cases} \dfrac{w_{m_1}^{s_1}}{w_1^0} = \dfrac{(2m_1-1)}{1-\eta_2}; & \text{when: } 2m \le \dfrac{w_{m_1}^{s_1}}{w_1^0} \le 2m+2 \\ \dfrac{w_{m_2}^{s_2}}{w_1^0} = \dfrac{(2m_2-1)}{\eta_2}; & \text{when: } 2m \le \dfrac{w_{m_2}^{s_2}}{w_1^0} \le 2m+2 \end{cases} \tag{B3}$$

where, just for clarity, m_1 and m_2 are introduced as mode numbers for the uncoupled subsystem 1 and subsystem 2, respectively. Changing the conditions in Eq. (B3) in terms of η_2 yields:

$$\frac{w_m^d}{w_1^0} = \begin{cases} \dfrac{w_{m_1}^{s_1}}{w_1^0} = \dfrac{(2m_1+1)}{1-\eta_2}; & \text{when: } 0 \le 1 - \dfrac{(2m_1+1)}{2m} \\ \le \eta_2 \le 1 - \dfrac{(2m_1+1)}{(2m+2)} \le 1 & \\ \dfrac{w_{m_2}^{s_2}}{w_1^0} = \dfrac{(2m_2+1)}{\eta_2}; & \text{when: } 0 \le \dfrac{(2m_2+1)}{(2m+2)} \\ \le \eta_2 \le \dfrac{(2m_2+1)}{2m} \le 1 & \end{cases} \tag{B4}$$

Notation

a = acoustic wave speed in water (m s^{-1})
A_0 = area of intact pipe (m^2)
A_2 = area of pipe with reduced cross sectional area (m^2)
C = complex integration constant (Pa)
$\overline{T}$ = normalized kinetic energy (–)
$\overline{U}$ = normalized elastic potential energy (–)
T = kinetic energy per unit length (J m^{-1})
U = elastic potential energy per unit length (J m^{-1})
E = total energy per unit length (J m^{-1})
g = acceleration due to gravity (m s^{-2})
H = instantaneous pressure head (m)
$\overline{H}$ = mean pressure head (m)
h = unsteady pressure head due to wave (m)
h_m^{amp} = mth maximum complex amplitude of pressure head (m)
h^* = dimensionless pressure head at x-l_1 (–)
i = $\sqrt{-1}$ (–)
J_n = 0 or 1 and represents the number at nth binary position of j (–)
j = counting numbers (–)
k = wavenumber (rad m^{-1})
k_m^s = mth wavenumber when$\alpha = 0$ (rad m^{-1})
$k_m^{\max}$ = mth wavenumber at maximum shift (rad m^{-1})
L = whole pipe length (m)
l_1 = length of pipe 1 (m)
l_2 = length of pipe 2 (m)
m = mode number for pipe system of length L (–)
τ = τth zero shift position at a given m mode (–)
N = number of blockages (–)
n = nth shift region between two consecutive zero shit locations at a given m mode (–)
M = 2^{N-1} (–)
m_1 = mode number for subsystem 1 (–)
m_2 = mode number for subsystem 2 (–)
P = pressure (Pa)
Q = instantaneous flow discharge (m^3 s^{-1})
$\overline{Q}$ = mean discharge (m^3 s^{-1})
q = unsteady discharge due to wave (m^3 s^{-1})
q_m^{amp} = mth maximum complex amplitude of flow discharge (m)
q^* = dimensionless discharge at $x - l_1$ (–)
S = total number of junctions between blockages and the unblocked section (–)
t = time (s)
V = unsteady flow velocity due to the wave (m s^{-1})
w = angular frequency (rad s^{-1})
w_m = mth resonant frequencies in the blocked pipe case (rad s^{-1})
w_m^0 = mth resonant frequencies in the intact pipe case (rad s^{-1})
w_m^s = mth eigenfrequency when$\alpha = 0$ (rad s^{-1})
$w_m^{s_1}$ = mth eigenfrequency of uncoupled subsystem 1 ($\alpha = 0$) (rad s^{-1})
$w_m^{s_2}$ = mth eigenfrequency of uncoupled subsystem 2 ($\alpha = 0$) (rad s^{-1})

x = axial coordinate (m)
Z = impedance (Pa m^{-3} s^{-1})
α = area ratio between A_2 and A_0 (–)
ΔE = energy change due to cross sectional area variation (J m^{-1})
$\overline{\Delta E}$ = integrated energy change over the pipe domain (J)
Δw_m = mth eigenfrequency shift (rad s^{-1})
$\Delta w_m^{\max}$ = maximum mth eigenfrequency shift (rad s^{-1})
$\overline{\Delta w_m}$ = mth integrated eigenfrequency shift over the pipe domain (rad s^{-1})
δk = small perturbation in wave number (rad m^{-1})
δw = small perturbation in eigenfrequency (rad s^{-1})
η_1 = l_1 / L dimensionless length (–)
η_2 = l_2 / L dimensionless length (–)
λ = probing wave length (m)
ν = counting numbers (–)
ξ = counting numbers (–)

References

Beyer, R. T. (1978). Radiation pressure—the history of a mislabeled tensor. *The Journal of the Acoustical Society of America*, *63*(4), 1025–1030.

Borgnis, F. E. (1953). Acoustic radiation pressure of plane compressional waves. *Reviews of Modern Physics*, *25*(3), 653–664. doi:10.1103/RevModPhys.25.653

Chaudhry, M. H. (2014). *Applied hydraulic transients* (3rd ed.). New York, NY: Springer.

De Salis, M. H. F., & Oldham, D. J. (1999). Determination of the blockage area function of a finite duct from a single pressure response measurement. *Journal of sound and vibration*, *221*(1), 180–186.

Domis, M. A. (1979). Acoustic resonances as a means of blockage detection in sodium cooled fast reactors. *Nuclear Engineering and Design*, *54*, 125–147.

Domis, M. A. (1980). Frequency dependence of acoustic resonances on blockage position in a fast reactor subassembly wrapper. *Journal of sound and vibration*, *72*(4), 443–450.

Duan, H. F., Lee, P. J., Ghidaoui, M. S., & Tung, Y. K. (2012). Extended blockage detection in pipelines by using the system frequency response analysis. *Journal of Water Resources Planning and Management, ASCE*, *138*(1), 55–62.

Duan, H. F., Lee, P. J., Kashima, A., Lu, J. L., Ghidaoui, M. S., & Tung, Y. K. (2013). Extended blockage detection in pipes using the system frequency response: Analytical analysis and experimental verification. *Journal Hydraulic Engineering ASCE*, *139*(7), 763–771.

Ehrenfest, P. (1916). On adiabatic changes of a system in connection with the quantum theory. *Proceedings of the Amsterdam Academy*, *19*, 576–597.

El-Rahed, M., & Wagner, P. (1982). Acoustic propagation in rigid ducts with blockage. *The Journal of the Acoustical Society of America*, *72*, 1046–1055.

Fant, G. (1975). Vocal-tract area and length perturbations. *STL-QPSR*, *16*(4), 1–14.

Ghidaoui, M. S. (2004). On the fundamental equations of water hammer. *Urban Water Journal*, *1*(2), 71–83.

Heinz, J. (1967). Perturbation functions for the determination of vocal-tract area functions from vocal-tract eigenvalues. *STL-QPSR*, *8*(1), 1–14.

Karney, B. W. (1990). Energy relations in transient closed-conduit flow. *Journal of Hydraulic Engineering*, *116*(10), 1180–1196.

Lanczos, C. (2012). *The variational principles of mechanics*. Mineola, NY: Courier Corporation. (Reprint).

Lee, P. J., Duan, H. F., Ghidaoui, M., & Karney, B. (2013). Frequency domain analysis of pipe fluid transient behaviour. *Journal of hydraulic research*, *51*(6), 609–622.

Lee, P. J., Vítkovský, J. P., Lambert, M. F., Simpson, A. R., & Liggett, J. (2008). Discrete blockage detection in pipelines using the frequency response diagram: numerical study. *Journal Hydraulic Engineering ASCE*, *134*(5), 658–663.

Lighthill, M. J. (1978). *Waves in fluids*. Cambridge, UK: Cambridge University Press.

Louati, M. (2013). *On wave-defect interaction in pressurized conduits*. *Proceedings of the 35th IAHR Congress*, Chengdu-China.

Louati, M., & Ghidaoui, M. S. (2015). *Role of length of probing waves for multi-scale defects detection in pipes*. *Proceedings of the 36th IAHR Congress*, The Hague-Netherland.

Mei, C. C., Stiassnie, M., & Yue, D. K. (2005). *Theory and applications of ocean surface waves*. Hackensack, NJ: World Scientific.

Meniconi, S., Duan, H. F., Lee, P. J., Brunone, B., Ghidaoui, M. S., & Ferrante, M. (2013). Experimental investigation of coupled frequency and time-domain transient test-based techniques for partial blockage detection in pipelines. *Journal Hydraulic Engineering ASCE*, *139*(10), 1033–1040.

Mermelstein, P. (1967). Determination of the vocal-tract shape from measured formant frequencies. *The Journal of the Acoustical Society of America*, *41*(5), 1283–1294.

Milenkovic, P. (1984). Vocal tract area functions from two point acoustic measurements with formant frequency constraints. *IEEE Transactions on Acoustics, Speech, and Signal Processing*, *32*(6), 1122–1135.

Milenkovic, P. (1987). Acoustic tube reconstruction from non-causal *excitation. IEEE Transactions on Acoustics, Speech, and Signal Processing*, *35*(8), 1089–1100.

Mohapatra, P. K., Chaudhry, M. H., Kassem, A. A., & Moloo, J. (2006). Detection of partial blockage in single pipelines. *Journal Hydraulic Engineering ASCE*, *132*(2), 200–206.

Nixon, W., & Ghidaoui, M. S. (2007). Numerical sensitivity study of unsteady friction in simple systems with external flows. *Journal of Hydraulic Engineering*, *133*(7), 736–749.

Qunli, W., & Fricke, F. (1989). Estimation of blockage dimensions in a duct using measured eigenfrequency shifts. *Journal of Sound and Vibration*, *133*(2), 289–301.

Qunli, W., & Fricke, F. (1990). Determination of blocking locations and cross-sectional area in a duct by eigenfrequency shifts. *The Journal of the Acoustical Society of America*, *87*(1), 67–75.

Sattar, A. M., Chaudhry, M. H., & Kassem, A. A. (2008). Partial blockage detection in pipelines by frequency response method. *Journal Hydraulic Engineering ASCE*, *134*(1), 76–89.

Schroeder, M. R. (1967). Determination of the geometry of the human vocal tract by acoustic measurements. *The Journal of the Acoustical Society of America*, *41*(4B), 1002–1010.

Schroeter, J., & Sondhi, M. M. (1994). Techniques for estimating vocal-tract shapes from the speech signal. *IEEE Transactions on Speech and Audio Processing*, *2*(1), 133–150.

Sondhi, M. M., & Gopinath, B. (1971). Determination of vocal-tract shape from impulse response at the lips. *The Journal of the Acoustical Society of America*, *49*(6B), 1867–1873.

Sondhi, M. M., & Resnick, J. (1983). The inverse problem for the vocal tract: Numerical methods, acoustical experiments, and speech synthesis. *The Journal of the Acoustical Society of America*, *73*(3), 985–1002.

Stevens, K. N. (1998). *Acoustic phonetics*. London: MIT press.

Wang, X. J., Lambert, M. F., & Simpson, A. R. (2005). Detection and location of a partial blockage in a pipeline using damping of fluid transients. *Journal of Water Resources Planning and Management, ASCE*, *131*(3), 244–249.

Zhao, M., Ghidaoui, M. S., Louati, M. & Duan, H. F. (in press). Transient wave and extended blockage interaction in pipe. *Journal of Hydraulic Research, IAHR*.